

Pulsars identified from the NRAO VLA Sky Survey

J.L. Han^{1,2,3} and W.W. Tian^{1,3}

¹ Beijing Astronomical Observatory, Chinese Academy of Sciences (CAS), Beijing 100012, China

² Beijing Astronomy Center, CAS-PKU, Beijing 100871, China

e-mail: jhan@bac.pku.edu.cn

³ Max-Planck-Institut für Radioastronomie, Auf dem Hügel 69, D-53121 Bonn, Germany

Received June 26, 1997; accepted March 1, 1999

Abstract. We identified 97 strong pulsars from the NRAO VLA Sky Survey (NVSS) at 1.4 GHz north of Dec(J2000) = -40° . The total flux density, linear polarization intensity and polarization angle (PA) of all pulsars are extracted from the NVSS catalog. The well-calibrated PA measurement of 5 pulsars can be used for absolute PA calibrations in other observations. Comparing the source positions with those in the pulsar catalog, we got the first measurement of the proper motion upper limit of PSR B0031–07, which is $\mu_\alpha \cos \delta = -102 \pm 74$ mas yr⁻¹ and $\mu_\delta = -105 \pm 78$ mas yr⁻¹.

Key words: pulsars: general — polarization — surveys

1. Introduction

Compared with other types of radio sources, pulsars are known to have strong polarization, even up to 100% if one observes them with high time resolutions. Pulsar polarization would be smeared somehow if they are observed as continuum point sources over a duration much longer than a pulsar period, mainly because of the fast swing of polarization angle across a pulse profile. However, we will show in this paper that is not so serious as generally believed.

Pulsars have high (birth) velocities, on average 450 km s⁻¹ (Lyne & Lorimer 1994) and maybe up to 1600 km s⁻¹ for individuals (e.g. Cordes & Chernoff 1998), much faster than that of other types of stars (typically a few tens km s⁻¹). The high velocity was probably caused by the asymmetric kick during supernova explosion when a pulsar was born. This leads to a large proper motion for (nearby) pulsars. However, measuring the proper motion is not an easy task since the precise positions of a pulsar at well-separated epochs have to be measured.

Up to now, there are 96 pulsars with proper motion measurements (e.g. Taylor et al. 1993; Fomalont et al. 1997).

Recently, the National Radio Astronomical Observatory (NRAO) Very Large Array (VLA) Sky Survey (NVSS) has been finished, which covers the sky north of Dec(J2000) = -40° at 1.4 GHz (Condon et al. 1998). The survey detected more than 1.8 million sources, with polarization measurements, down to a flux density limit about 2.5 mJy. Observations have a resolution of 45", but the positional accuracy is a few arcsec for weak sources, and much better for strong sources. The observations were made with two IF channels at 1.365 and 1.435 GHz with an effective bandwidth of 42 MHz each. Most sources in the NVSS were observed in three pointings of 23 s each. The final sky map is the weighted sum from these pointings (Condon et al. 1998).

We had tried to identify the pulsars from the NVSS catalog, and then to investigate the pulsar polarization properties and proper motions from continuum observations. In the sky region covered by the NVSS, there are 520 known pulsars according to the updated pulsar catalog of Taylor et al. (1993). Updated catalog was kindly provided by Manchester. Using the latest version of the NVSS catalog (with 1814748 entries), we identified 97 strong pulsars according to positional coincidence. During revising this paper for publication, we noticed that similar identification work has been done by Kaplan et al. (1998), but they emphasized the other aspects, such as position accuracy, scintillation effects and completeness of detections. Comparing to Kaplan et al. (1998), we got 24 further new identifications. In the following, we will not repeat their work, but present our results in Sect. 2. We discuss briefly in Sect. 3 about scintillations (Sect. 3.1), pulsar polarization properties (Sect. 3.2), and proper motions (Sect. 3.3). We compared the pulsar positions with those from the pulsar catalog if the epochs were separated over more than 5 years, and got the upper limits of proper motion of 18

pulsars, including one pulsar which has had no proper motion measurements previously.

2. Identification and results

We took positions of pulsars from the updated catalog of Taylor et al. (1993). PSR names in J2000, and B1950 if applicable, are given in the Cols. (1) and (2) of the Table 1. Their positions are given in Cols. (3) and (4), generally with an accuracy better than $0.1''$, but occasionally up to a few arcsec. These positions were determined by timing observations or interferometric measurements at epoch for the position¹ in Col. (5). For comparison, we list in Col. (6) the flux density at 1.4 GHz from pulsar catalog, which were normally obtained from the average of several pulsar observation sessions to overcome scintillation effects. We searched for radio sources in the NVSS catalog within $30''$ angular distance around each of the 520 pulsar positions. Only 106 radio sources were found to match the positions and are probably pulsars. The positions of the NVSS sources are listed in Cols. (7) and (8). The angular offset from pulsar positions “ Δ ” in arcsec is given in Col. (9). The flux density and polarization parameters of the NVSS sources extracted from the NVSS catalog are listed in Cols. (10)–(13). A blank in these columns indicates no significant detection above the sensitivity limit of linear polarization of the NVSS (~ 0.5 mJy). We marked in Col. (14) if there was any further consideration during identification.

Note that the epochs for pulsar position in the pulsar catalog differ from that of NVSS observations. However, even if a pulsar has the largest proper motion, e.g. 400 mas per year, then after 20 years, the position offset would be $8''$. So, our search in $30''$ should not miss any known pulsar if it is detectable by the NVSS².

On the other hand, the NVSS was done over a long period, from ~ 1993 to ~ 1996 . We will take an approximate epoch MJD 49718 (~ 1995.0) in following discussion. There should be only a very small position offset ($< 1''$) caused by pulsar proper motions, if any, over the NVSS observation period, much smaller than the position uncertainties of the NVSS sources listed in Table 1. If the position of a pulsar was measured at an epoch later than MJD 47000, we will not consider its proper motion during the identification process for the same reason.

¹ There are two epochs in the pulsar catalog, one (“epoch”) for pulsar period and period derivatives and the other (“epoch”) for pulsar position. If “epoch” was not available, we used the “pepoch” as instructed by Manchester (private communications).

² We missed 4 pulsars which appear in Table 1 of Kaplan et al. (1998): PSRs B1823-11, B1900-06, B1901+10, and B2323+63. Their position offsets to the NVSS sources or position uncertainties are too large ($> 30''$) to make significant assessment. For the same reason, we removed J1848+0651 from our sample which was included by Kaplan et al. (1998).

The first step for identification is to check the position offset Δ . At this stage, we ignored the proper motion. If Δ is smaller than twice of the total position uncertainty, i.e. $\Delta \lesssim 2\sqrt{\sigma_{\text{nvss}}^2 + \sigma_{\text{psrcat}}^2}$, then we attribute the NVSS source as being a positive identification of a pulsar. This process yielded the first 90 positive detections. If any pulsar position was obtained at an epoch several years ago, the pulsar must have had only a very small proper motion so that the position offsets are not significant.

Now we consider the remaining 16 sources more carefully, which are marked with “?” in Col. (14) of Table 1.

Nine Confusion cases: (a) PSR B0531+21 (Crab) and PSR B1951+32 are confused by their associated supernova remnants. We marked them in Notes, i.e. Col. (14), of Table 1 with “SNR”. (b) PSRs B1112+50, B1829-10 and B1831-00 are confused by their nearby strong sources which have much larger flux density (more than 10 times) than that from the pulsar catalog. One NVSS source was detected $28.1''$ (formally 7.8σ) away from PSR B1920+21, too large to be proper motion for this distant pulsar (distance ~ 12.5 kpc). We consider these detections unlikely and mark with “no” in Notes to stand for “no detection”. (c) PSRs B1744-24A and J2129+1210A, (maybe also B1745-20 as indicated by Kaplan et al. 1998), are confused by other continuum sources in the host globular clusters Terzan-5 and M 15, (and NGC 6440?), respectively. They are marked with “glbc”. (d) PSR B1718-35 is a marginal case, maybe confused by a source $19.4''$ away, with 4.7σ for position offset and 27.7 mJy in flux (pulsar: 10.0 mJy).

Seven detection cases: (a) The position offset of the NVSS source to PSR B1831-04 is only $4.75''$ (formally 2.3σ , or 2.6σ rather than 14σ using the new position in Kaplan et al. 1998), much smaller than the beam size of the NVSS. Although Kaplan et al. (1998) suggested otherwise, we believe the pulsar is detected. The consistent flux densities of the pulsar and the NVSS source confirm the identification. We mark such a case as “yes” in the Notes. (b) PSRs B0823+26, B1133+16, B2016+28, (and B2154+40) have small position offsets caused by proper motions (see Sect. 3.3). (c) PSR B1820-31 is detected with a position offset of $12.5'' = 2.6\sigma$, as confirmed by consistent flux density, and more importantly, by the highly linear polarization of the NVSS source. (d) A marginal case is the strong pulsar PSR B2020+28. The NVSS survey detected a very weak source 2.2σ away, too weak to believe the identification (see more discussion below). However, highly linear polarization of the source suggests that it is the pulsar. We mark in the Notes “yes?” for this case.

In all, the NVSS detected 97 pulsars, including the 73 which appeared in Kaplan et al. (1998) and 24 new identifications³ marked with “*” in the Notes.

³ The PSR J1615-39 in Table 1 of Kaplan et al. (1998) is missing from the pulsar catalog available to us.

Table 1. NVSS sources around pulsar positions

(1) PSR J	(2) PSR B	(3) RA(2000) h m s	(4) Dec(2000) ° ′ ″	(5) Epoch MJD	(6) SI.4 mJy	(7) RA(2000)nvss h m s	(8) Dec(2000)nvss ° ′ ″	(9) Δ ('')	(10) $S_{1.4} \pm \sigma$ (mJy)	(11) $L_{1.4} \pm \sigma$ (mJy)	(12) L/S (%)	(13) PA $\pm \sigma$ (deg)	(14) Notes
0014+4746	0011+47	00 14 17.74.06	47 46 33.1 0.6	48416	3.0	00 14 18.18.044	+47 46 39.7 4.5	7.97	4.9 \pm 0.5	1.95 \pm 0.60	40 \pm 13	24 \pm 6	
0034-0721	0031-07	00 34 08.88.03	-07 21 53.4 0.7	40690	11.0	00 34 08.71.012	-07 21 56.0 1.8	3.66	14.6 \pm 1.1	0.89 \pm 0.61	6 \pm 4	-11 \pm 14	
0055+5117	0052+51	00 55 45.39.03	51 17 24.8 0.3	46116	1.5	00 55 45.12.119	+51 17 22.9 5.1	3.19	4.1 \pm 0.4	1.34 \pm 0.83	33 \pm 20	0 \pm 10	
0139+5814	0136+57	01 39 19.77.00	58 14 31.8 0.0	48382	4.6	01 39 19.99.046	+58 14 37.4 5.0	5.90	4.0 \pm 0.4	2.09 \pm 0.56	52 \pm 15	-22 \pm 5	
0141+6009	0138+59	01 41 39.95.00	60 09 32.3 0.0	46573	4.5	01 41 39.73.041	+60 09 26.5 3.2	6.06	5.4 \pm 0.4	1.11 \pm 0.57	21 \pm 11	-3 \pm 10	*
0304+1932	0301+19	03 04 33.11.01	19 32 50.7 0.1	46058	3.0	03 04 33.04.015	+19 32 47.6 2.2	3.20	6.4 \pm 0.5	0.42 \pm 0.38	7 \pm 6	
0332+5434	0329+54	03 34 43.2 0.1	54 34 43.2 0.1	40105	203	03 34 44.1 0.6	+54 34 44.1 0.6	1.12	150.7 \pm 5.4	5.52 \pm 0.53	4 \pm 0	44 \pm 2	
0357+5236	0353+52	03 57 44.82.00	52 36 57.7 0.1	48416	1.9	03 57 44.53.068	+52 36 51.5 7.9	6.72	3.2 \pm 0.5	1.08 \pm 0.69	34 \pm 22	
0358+5413	0355+54	03 58 53.70.00	54 13 13.6 0.0	46573	23.0	03 58 53.89.016	+54 13 15.9 1.6	2.85	10.3 \pm 0.5	3.57 \pm 0.49	35 \pm 5	19 \pm 3	
0406+6138	0402+61	04 06 30.05.01	61 38 40.7 0.2	48416	2.8	04 06 30.27.127	+61 38 30.7 10.1	10.1	3.7 \pm 0.4	0.11 \pm 0.91	3 \pm 25	
0452-1759	0450-18	04 52 34.10.00	-17 59 23.5 0.1	46573	5.3	04 52 34.02.007	-17 59 21.2 1.0	2.56	14.5 \pm 0.6	1.76 \pm 0.40	12 \pm 3	-75 \pm 5	*
0454+5543	0450+55	04 54 07.62.00	55 43 41.2 0.1	46460	13.0	04 54 07.47.022	+55 43 41.4 2.3	1.25	7.8 \pm 0.5	1.75 \pm 0.47	22 \pm 6	-54 \pm 7	
0528+2200	0525+21	05 28 52.34.02	22 00 00.2 5.0	41994	9.0	05 28 52.26.065	+22 00 06.8 13.6	6.72	2.8 \pm 0.5	1.53 \pm 0.96	19 \pm 12	
0534+2200	0531+21	05 34 31.97.01	22 00 52.1 0.1	40675	14.0	05 34 31.56.033	+22 00 43.2 0.6	21.5	4106 \pm 123	99.9 \pm 0.54	90 \pm 0	? :SNR
0538+2817	05 38 25.06.04	28 17 11.0 5.0	49444	05 38 25.11.029	+28 17 17.7 4.4	6.73	4.2 \pm 0.5	2.95 \pm 0.62	70 \pm 17	-58 \pm 5	
0543+2329	0540+23	05 43 09.65.00	23 29 06.1 0.0	47555	9.0	05 43 09.66.011	+23 29 04.1 1.7	1.93	15.8 \pm 1.4	7.38 \pm 0.72	47 \pm 6	-25 \pm 2	
0629+2415	0626+24	06 29 05.72.00	24 15 41.6 0.1	47555	3.2	06 29 05.74.023	+24 15 38.3 3.2	3.34	4.7 \pm 0.5	
0630-2834	0628-28	06 30 49.53.01	-28 34 43.6 0.1	40585	23.0	06 30 49.61.009	-28 34 41.8 1.2	2.04	13.8 \pm 0.6	4.01 \pm 0.44	29 \pm 3	-31 \pm 2	
0742-2822	0740-28	07 42 49.07.00	-28 22 44.0 0.1	46573	23.0	07 42 49.03.006	-28 22 42.7 0.8	1.46	22.3 \pm 0.8	13.44 \pm 0.45	60 \pm 3	-33 \pm 1	
0814+7429	0809+74	08 14 59.44.04	74 29 05.8 0.1	48382	10.0	08 14 58.88.062	+74 29 05.7 2.2	2.23	7.7 \pm 0.5	2.65 \pm 0.50	34 \pm 7	-45 \pm 4	
0820-1350	0818-13	08 20 26.36.01	-13 50 55.2 0.1	46573	7.0	08 20 26.38.021	-13 50 53.4 3.1	1.80	5.5 \pm 0.5	0.29 \pm 0.45	5 \pm 8	
0826+2637	0823+26	08 26 51.31.00	26 37 25.6 0.1	40264	10.0	08 26 51.40.007	+26 37 21.9 1.0	3.88	17.1 \pm 0.7	2.24 \pm 0.44	13 \pm 3	75 \pm 4	? :yes
0837+0610	0834+06	08 37 05.65.00	06 10 14.1 0.1	46058	4.0	08 37 04.24.039	+06 10 13.4 8.2	21.0	3.2 \pm 0.4	0.52 \pm 0.64	14 \pm 17	
0846-3533	0844-35	08 46 05.86.14	-35 33 39.9 1.5	43557	4.0	08 46 05.64.037	-35 33 31.2 5.8	9.12	3.7 \pm 0.5	0.39 \pm 0.50	12 \pm 16	
0922+0638	0919+06	09 22 13.98.00	06 38 21.6 0.0	46573	4.2	09 22 14.39.017	+06 38 24.3 2.5	6.69	6.9 \pm 0.5	3.81 \pm 0.47	55 \pm 8	41 \pm 2	
0953+0755	0950+08	09 53 09.32.00	07 55 35.6 0.0	46058	84.0	09 53 09.31.003	+07 55 36.9 0.6	1.30	92.0 \pm 2.8	2.78 \pm 0.42	3 \pm 0	-14 \pm 4	
1012+5307	10 12 33.43.00	53 07 02.6 0.0	49220	2.8	10 12 33.31.036	+53 07 04.9 4.8	2.58	4.5 \pm 0.4	1.95 \pm 0.48	43 \pm 11	-17 \pm 5	
1022+1001	10 22 58.05.06	10 01 54.0 3.0	49780	2.3	10 22 57.92.034	+10 01 53.5 9.2	2.00	3.5 \pm 0.4	1.46 \pm 0.61	42 \pm 18	9 \pm 8	
1034-3224	10 34 19.48.01	-32 24 26.3 0.1	49020	4.7	10 34 19.18.026	-32 24 23.3 4.2	4.83	4.4 \pm 0.5	*
1115+5030	1112+50	11 15 38.35.02	50 30 13.5 0.3	44240	3.0	11 15 38.56.006	+50 30 25.6 0.7	12.2	35.2 \pm 1.1	0.19 \pm 0.38	1 \pm 1	? :no
1136+1551	1133+16	11 36 03.30.00	15 51 00.7 0.1	42364	32.0	11 36 03.28.005	+15 51 06.9 0.8	6.16	21.2 \pm 0.8	1.54 \pm 0.39	7 \pm 2	-57 \pm 6	? :yes
1239+2453	1237+25	12 39 40.47.00	24 53 49.3 0.0	46460	10.0	12 39 48.3 0.9	+24 53 48.3 0.9	1.16	20.5 \pm 0.7	7.49 \pm 0.38	37 \pm 2	84 \pm 1	mode
1320-3512	13 20 12.70.10	-35 12 24.0 2.0	48734	8.0	13 20 12.58.015	-35 12 24.1 2.0	1.51	7.9 \pm 0.5	1.28 \pm 0.47	16 \pm 6	60 \pm 7	*
1509+5531	1508+55	15 09 25.72.01	55 31 33.0 0.1	48383	8.0	15 09 25.78.023	+55 31 34.6 2.0	1.74	7.7 \pm 0.5	1.03 \pm 0.40	13 \pm 5	8 \pm 9	
1518+4904	15 18 16.60.10	49 04 35.0 1.0	15 18 17.08.042	+49 04 30.9 4.6	6.26	4.4 \pm 0.4	0.12 \pm 0.48	3 \pm 11	*
1543+0929	1541+09	15 43 38.83.01	09 29 16.8 0.2	42304	5.9	15 43 38.88.010	+09 29 14.8 1.5	2.10	10.0 \pm 0.5	1.72 \pm 0.47	17 \pm 5	64 \pm 6	*
1543-0620	1540-06	15 43 30.17.01	-06 20 45.3 0.1	46573	2.0	15 43 30.33.043	-06 20 46.8 6.8	2.84	2.8 \pm 0.5	*
1603-2531	16 03 04.88.00	-25 31 48.3 0.1	49408	5.0	16 03 04.97.061	-25 31 47.9 6.8	1.21	3.1 \pm 0.5	0.80 \pm 0.81	26 \pm 26	*
1607-0032	1604-00	16 07 12.12.00	-00 32 40.2 0.1	42307	5.0	16 07 12.00.027	-00 32 48.8 5.7	8.73	4.1 \pm 0.5	*
1643-1224	16 43 38.15.00	-12 24 58.7 0.0	49524	3.1	16 43 38.60.025	-12 24 51.8 3.7	9.50	3.9 \pm 0.4	0.10 \pm 0.47	3 \pm 12	*
1645-0317	1642-03	16 45 02.03.00	-03 17 58.3 0.1	40414	21.0	16 45 02.34.040	-03 18 10.5 7.1	13.1	8.3 \pm 1.5	*
1700-3312	17 00 53.02.01	-33 12 45.1 0.6	49424	17.0	17 00 52.52.047	-33 12 59.8 6.7	16.0	2.8 \pm 0.5	0.72 \pm 0.77	26 \pm 28	*
1703-3241	1700-32	17 03 22.37.12	-32 41 45.2 3.5	48000	6.0	17 03 22.34.025	-32 41 51.6 2.7	6.45	6.7 \pm 0.5	1.23 \pm 0.85	18 \pm 13	*
1705-1906	1702-19	17 05 36.11.01	-19 06 38.5 0.7	48331	8.0	17 05 36.04.010	-19 06 38.9 3.9	3.98	5.6 \pm 0.5	2.82 \pm 0.68	50 \pm 13	-39 \pm 7	
1705-3423	17 05 42.37.00	-34 23 44.5 0.2	49500	17.0	17 05 42.30.038	-34 23 41.2 5.6	3.40	4.2 \pm 0.5	2.14 \pm 0.67	51 \pm 17	-85 \pm 15	*
1708-3426	17 08 57.75.01	-34 26 47.5 0.8	49339	2.4	17 08 58.33.047	-34 26 33.7 1.1	15.5	2.9 \pm 0.5	1.42 \pm 0.74	49 \pm 27	-23 \pm 14	*
1713+0747	17 13 49.52.00	07 47 37.5 0.0	49056	3.0	17 13 50.11.049	+07 47 38.4 3.9	8.81	8.0 \pm 1.4	*
1721-3532	1718-35	17 21 32.80.02	-35 32 46.6 0.9	48379	10.0	17 21 34.60.030	-35 32 58.5 3.7	19.2	27.7 \pm 2.1	2.42 \pm 0.99	9 \pm 4	13 \pm 20	? :no?
1733-2228	1730-22	17 33 26.41.06	-22 28 36.4 1.6	48417	2.2	17 33 26.04.010	-22 28 39.9 4.1	4.37	3.2 \pm 0.4	0.27 \pm 0.59	8 \pm 18	*
1740+1311	1737+13	17 40 07.37.02	13 11 57.5 0.3	43893	3.9	17 40 07.29.046	+13 11 57.9 7.2	1.29	3.8 \pm 0.5	0.47 \pm 0.86	12 \pm 23	*
1741-0840	1738-08	17 41 22.54.03	-08 40 32.7 1.6	48417	1.4	17 41 22.48.032	-08 40 29.7 6.3	3.11	3.3 \pm 0.5	0.70 \pm 0.61	21 \pm 19	*
1741-3927	1737-39	17 41 18.04.03	-39 27 37.8 1.4	43558	3.5	17 41 17.42.031	-39 27 45.0 4.7	10.2	4.5 \pm 0.5	*
1744-1134	17 44 29.39.00	-11 34 54.6 0.0	49882	1.0	17 44 29.31.030	-11 34 58.6 5.5	4.18	3.8 \pm 0.5	2.99 \pm 0.75	79 \pm 22	48 \pm 5	*
1745-3040	1742-30	17 45 56.30.00	-30 40 23.6 0.3	46956	14.0	17 45 56.28.017	-30 40 28.6 2.5	5.02	6.6 \pm 0.5	5.96 \pm 0.44	90 \pm 10	-38 \pm 2	
1748-1300	1745-12	17 48 17.37.04	-13 00 53.3 2.0	43891	2.0	17 48 17.54.030	-13 00 39.6 8.6	14.0	4.4 \pm 0.5	*

Table 1. continued

(1) PSR J	(2) PSR B	(3) RA(2000) h m s σ	(4) Dec(2000) $^{\circ}$ ' " σ	(5) Epoch MJD σ	(6) $S_{1.4}$ mJy	(7) RA(2000)nvss h m s σ	(8) Dec(2000)nvss $^{\circ}$ ' " σ	(9) Δ (")	(10) $S_{1.4} \pm \sigma$ (mJy)	(11) $L_{1.4} \pm \sigma$ (mJy)	(12) L/S (%)	(13) $PA \pm \sigma$ (deg)	(14) Notes
1748-2021	1745-20	17 48 52.61 .10	-20 21 40.1 3.0	49215	1.5	17 48 53.14 0.43	-20 21 34.6 9.3	9.24	4.5 \pm 0.5	0.74 \pm 1.14	16 \pm 25	
1748-2446A	1744-24A	17 48 02.25 .00	-24 46 37.7 0.5	48270	2.5	17 48 04.37 0.39	-24 46 41.5 4.6	29.1	3.7 \pm 0.5	2.24 \pm 0.65	61 \pm 19	-84 \pm 7	?:glbc *
1750-3157	1747-31	17 50 47.29 .03	-31 57 41.3 3.0	48379	1.4	17 50 47.96 0.59	-31 58 01.3 1.0	21.7	3.5 \pm 0.4	1.78 \pm 1.06	51 \pm 31	-78 \pm 24	*
1752-2806	1749-28	17 52 58.69 .00	-28 06 38.3 0.5	40352	36.0	17 52 58.82 0.04	-28 06 37.5 0.7	1.88	41.6 \pm 1.3	2.36 \pm 0.51	6 \pm 1	-16 \pm 5	
1801-2920	1758-29	18 01 46.83 .03	-29 20 37.1 3.0	48377	2.8	18 01 46.89 0.55	-29 20 33.0 7.2	4.16	2.2 \pm 0.5	1.84 \pm 0.62	84 \pm 34	-66 \pm 14	
1807-0847	1804-07	18 07 38.02 .01	-08 47 43.1 0.2	46573	16.0	18 07 38.08 0.12	-08 47 41.5 2.0	1.83	9.6 \pm 0.5	
1817-3618	1813-36	18 17 05.76 .02	-36 18 05.5 0.9	48426	2.0	18 17 05.44 0.44	-36 18 00.7 9.5	6.13	4.8 \pm 0.5	0.87 \pm 1.30	18 \pm 27	*
1820-0427	1818-04	18 20 52.62 .00	-04 27 38.5 0.1	40614	8.0	18 20 52.17 0.18	-04 27 37.0 2.7	6.87	5.9 \pm 0.5	
1822-2256	1819-22	18 22 58.96 .15	-22 56 49.3 5.4	48382	3.2	18 22 58.68 0.51	-22 56 31.0 8.5	18.7	4.0 \pm 0.5	
1823+0550	1821+05	18 23 30.98 .03	05 50 24.7 0.5	44240	1.7	18 23 31.17 0.33	+05 50 16.2 8.4	8.97	3.2 \pm 0.5	0.45 \pm 0.76	14 \pm 24	*
1823-3106	1820-31	18 23 46.78 .00	-31 06 49.7 0.2	48382	2.5	18 23 46.11 0.24	-31 06 40.7 3.7	12.5	4.9 \pm 0.5	2.60 \pm 0.65	53 \pm 14	89 \pm 7	?:yes
1824-1945	1821-19	18 24 00.45 .04	-19 45 50.7 8.0	46800	6.1	18 23 59.94 0.33	-19 45 49.1 3.6	7.30	5.1 \pm 0.5	
1825-0935	1822-09	18 25 30.60 .01	-09 35 22.8 0.4	48381	11.0	18 25 30.60 0.05	-09 35 21.7 0.9	1.10	29.2 \pm 1.4	9.43 \pm 0.66	32 \pm 3	-39 \pm 1	
1829-1751	1826-17	18 29 43.12 .01	-17 51 02.9 1.8	46944	10.3	18 29 43.12 0.13	-17 51 03.8 2.6	0.90	12.2 \pm 1.2	
1832-1021	1829-10	18 32 40.90 .01	-10 21 34.2 0.5	48000	0.6	18 32 40.58 0.16	-10 21 19.1 4.7	15.8	11.7 \pm 1.4	?:no
1834-0010	1831-10	18 34 17.24 .04	-00 10 49.5 0.9	46071	1	18 34 18.77 0.03	-00 10 55.2 0.6	23.7	70.6 \pm 2.2	0.31 \pm 0.64	?:no
1834-0426	1831-04	18 34 25.62 .02	-04 26 15.4 0.6	48000	15.0	18 34 25.48 0.08	-04 26 11.2 1.5	4.75	16.7 \pm 0.7	0.23 \pm 0.59	1 \pm 4	?:yes
1836-1008	1834-10	18 36 53.89 .09	-10 08 09.3 5.0	43893	5.0	18 36 52.99 0.61	-10 08 13.0 18.	13.8	4.3 \pm 0.5	*
1840+5640	1839+56	18 40 44.59 .05	56 40 55.5 0.4	48381	4.0	18 40 44.20 0.25	+56 40 55.8 2.3	3.21	10.0 \pm 1.0	2.69 \pm 0.56	27 \pm 6	31 \pm 4	
1841+0912	1839+09	18 41 55.97 .01	09 12 07.7 0.2	43890	1.7	18 41 56.35 0.46	+09 12 17.2 5.7	11.1	3.7 \pm 0.5	1.85 \pm 0.74	50 \pm 21	-21 \pm 13	
1857+0943	1855+09	18 57 36.39 .00	09 43 17.3 0.0	47526	4.0	18 57 36.27 0.35	+09 43 41.8 18.	24.6	3.8 \pm 0.5	
1900-2600	1857-26	19 00 47.60 .01	-26 00 48.1 0.3	46573	13.0	19 00 47.68 0.07	-26 00 44.8 1.1	2.02	17.8 \pm 0.7	1.99 \pm 0.60	11 \pm 3	-6 \pm 5	
1903+0135	1900+01	19 03 29.98 .00	01 35 38.2 0.1	42345	2.0	19 03 30.43 0.74	+01 35 33.3 8.5	8.28	4.3 \pm 0.6	
1910+0358	1907+03	19 10 09.08 .20	03 58 26.8 5.0	43984	4.0	19 10 09.73 0.55	+03 58 33.7 7.8	11.8	4.7 \pm 0.5	
1913-0440	1911-04	19 13 54.18 .01	-04 40 47.6 0.4	41902	4.4	19 13 54.37 0.21	-04 40 46.9 4.4	2.92	5.1 \pm 0.5	0.15 \pm 0.80	3 \pm 16	
1916+1312	1914+13	19 16 58.69 .01	13 12 49.7 0.3	48382	1.9	19 16 58.96 0.78	+13 12 49.4 16.	4.02	3.9 \pm 0.5	2.25 \pm 1.40	58 \pm 37	-35 \pm 15	
1922+2110	1920+21	19 22 53.55 .00	21 10 22.3 0.2	42546	1.4	19 22 52.26 0.18	+21 11 03.4 2.6	28.1	6.0 \pm 0.5	?:no
1932+1059	1929+10	19 32 13.90 .00	10 59 32.0 0.1	48381	41.0	19 32 14.03 0.05	+10 59 31.9 0.8	1.90	27.1 \pm 0.9	18.68 \pm 0.57	69 \pm 3	46 \pm 1	
1935+1616	1933+16	19 35 47.83 .00	16 16 40.6 0.0	40213	42.0	19 35 47.82 0.04	+16 16 39.7 0.7	0.91	43.3 \pm 1.4	7.76 \pm 0.53	18 \pm 1	-30 \pm 1	
1937+2544	1935+25	19 37 01.26 .01	25 44 13.7 0.1	48415	2.3	19 37 01.39 0.42	+25 44 15.9 5.7	2.75	2.8 \pm 0.5	0.63 \pm 0.51	23 \pm 19	
1946+1805	1944+17	19 46 53.04 .00	18 05 41.6 0.1	42320	10.0	19 46 53.00 0.37	+18 05 43.2 4.1	1.64	3.5 \pm 0.4	0.81 \pm 0.58	23 \pm 17	29 \pm 12	
1948+3540	1946+35	19 48 25.04 .00	35 40 11.3 0.0	42221	8.3	19 48 24.93 0.21	+35 40 08.2 2.9	3.44	5.9 \pm 0.5	1.40 \pm 0.57	24 \pm 10	81 \pm 11	*
1952+3252	1951+32	19 52 58.30 .01	32 52 40.4 0.2	47005	1.0	19 52 58.59 0.04	+32 52 43.3 0.6	4.71	97.9 \pm 36.	5.55 \pm 0.72	1 \pm 0	55 \pm 3	?:SNR
2018+2839	2016+28	20 18 03.85 .00	28 39 54.3 0.0	40105	30.0	20 18 04.11 0.06	+28 39 54.7 0.8	3.62	24.7 \pm 0.8	1.40 \pm 0.53	6 \pm 2	-58 \pm 10	?:yes *
2022+2854	2020+28	20 22 37.08 .00	28 54 23.5 0.0	42370	38.0	20 22 38.95 0.72	+28 54 19.1 8.1	24.9	3.6 \pm 0.5	2.21 \pm 1.01	61 \pm 29	57 \pm 11	?:yes? *
2022+5154	2021+51	20 22 49.90 .00	51 54 50.1 0.0	40614	27.0	20 22 49.85 0.10	+51 54 49.5 1.0	0.74	17.2 \pm 0.7	6.10 \pm 0.46	35 \pm 3	11 \pm 2	
2023+5037	2022+50	20 23 41.94 .01	50 37 34.8 0.0	48591	2.2	20 23 41.95 0.64	+50 37 39.9 5.7	5.10	7.4 \pm 1.4	0.99 \pm 0.98	13 \pm 13	*
2048-1616	2045-16	20 48 35.47 .00	-16 16 44.4 0.1	46573	13.0	20 48 35.69 0.14	-16 16 45.4 2.5	3.27	7.0 \pm 0.5	1.16 \pm 0.45	17 \pm 7	53 \pm 9	
2108+4441	2106+44	21 08 20.48 .01	44 41 48.8 0.1	48383	5.4	21 08 20.60 0.36	+44 41 48.8 3.6	1.30	4.7 \pm 0.5	0.27 \pm 0.44	6 \pm 9	*
2113+4644	2111+46	21 13 24.29 .01	46 44 08.7 0.1	48382	19.0	21 13 24.25 0.06	+46 44 08.6 0.7	0.56	37.6 \pm 1.5	4.07 \pm 0.50	11 \pm 1	-40 \pm 3	
2124-3358	21 24 43.86 .00	-33 58 44.2 0.0	49674	1.6	21 24 44.11 0.43	-33 58 35.2 1.1	9.56	3.0 \pm 0.5	0.14 \pm 0.68	4 \pm 23	?:glbc
2129+1210ABHE	2129+58.25	21 29 58.25 .01	12 10 01.3 0.1	47633	21.29	59.27 0.16	+12 10 14.1 3.5	~20	6.3 \pm 0.5	0.13 \pm 0.51	
2139+2242	21 39 27.00 .30	22 42 40.0 5.0	49542	22.42	40.0 5.0	+22 42 39.7 2.0	1.11	8.4 \pm 0.5	1.33 \pm 0.45	16 \pm 5	-45 \pm 8	
2145-0750	21 45 50.47 .00	-07 50 18.3 0.0	48979	10.0	21 45 50.71 0.13	-07 50 15.5 6.7	4.51	3.1 \pm 0.5	0.53 \pm 0.57	17 \pm 19	*
2157+4017	2154+40	21 57 01.81 .01	40 17 45.8 0.1	48382	17.0	21 57 02.07 0.07	+40 17 45.2 0.9	3.05	22.2 \pm 0.8	4.10 \pm 0.49	18 \pm 2	-11 \pm 3	?:yes
2215+1538	22 15 39.65 .00	15 38 34.9 0.1	49079	39.66 0.22	+15 38 35.7 2.6	1.68	6.0 \pm 0.4	1.82 \pm 0.50	30 \pm 9	22 \pm 6	
2219+4754	2217+47	22 19 48.13 .00	47 54 53.8 0.0	48382	3.0	22 19 47.32 0.59	+47 54 52.1 6.6	8.33	3.9 \pm 0.4	0.39 \pm 0.62	10 \pm 16	
2225+6535	2224+65	22 25 52.36 .02	65 35 33.0 0.1	48382	2.0	22 25 52.62 0.17	+65 35 38.1 7.0	4.58	4.9 \pm 0.5	2.38 \pm 1.01	49 \pm 21	76 \pm 6	
2313+4253	2310+42	23 13 08.57 .01	42 53 13.0 0.0	43891	15.0	23 13 08.32 0.18	+42 53 13.4 1.4	2.82	13.2 \pm 1.1	1.24 \pm 0.53	9 \pm 4	48 \pm 8	
2330-2005	2327-20	23 30 26.80 .02	-20 05 28.6 0.5	46916	3.0	23 30 26.49 0.37	-20 05 36.2 5.8	8.79	5.0 \pm 0.5	2.25 \pm 0.72	45 \pm 15	-27 \pm 8	
2354+6155	2351+61	23 54 04.70 .02	61 55 46.8 0.1	48382	5.0	23 54 05.27 0.72	+61 55 45.8 5.6	4.13	3.0 \pm 0.5	0.18 \pm 0.53	6 \pm 18	*

Notes ? : more considerations in texts; SNR: confused with supernova remnant; no: confused with a strong sources nearby; glbc: confused by host globular cluster; *: new identifications not presented by Kaplan et al. (1998); mode: PSR B1237+25 is in abnormal mode as comparing the PA with Fig. 7 of Bartel et al. (1982).

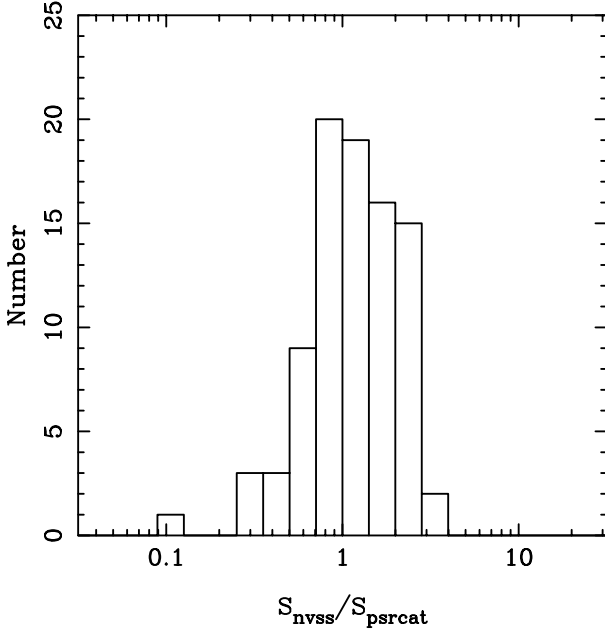


Fig. 1. The histogram for the flux comparison. Some pulsars (e.g. these in Table 1) have been missed in the left-half of the distribution (i.e. when $S_{nvss}/S_{psrct} < 1$), because scintillation makes them weaker than the NVSS sensitivity

3. Discussion

3.1. Scintillation and undetected pulsars

The VLA measurements of the flux densities $S_{1.4}$ of most identified pulsars, averaged over about 84 MHz bandwidth and 3×23 s in time, are comparable to the flux densities published in Lorimer et al. (1995) and Gould & Lyne (1998). They are generally within a factor of 2 of the published densities (see Fig. 1), but sometimes up to a factor of 3 or more. Most of undetected pulsars (~ 400) have flux densities below 2 or 3 mJy. Interstellar scintillation (e.g. Gupta et al. 1994) both helps and hinders the detections (Cordes & Lazio 1991). Some pulsars which have a flux density less than 2 mJy in the pulsar catalog have been detected in the NVSS with a larger flux density. The scintillation effect is more obvious for strong pulsars. For example, PSR B2020+28 should be as strong as 38.0 mJy, but in the NVSS it appears to be a highly polarized source of 3.6 ± 0.5 mJy. Among 61 pulsars with known flux densities larger than 5 mJy, about one fourth were missed by the NVSS (as listed in Table 2), some due to scintillation, some due to confusion (Condon, private communication).

3.2. Polarization

When pulsars are observed as continuum radio sources, the polarized intensity, L , and polarization position angle, PA, are calculated from the integrated Q and U values of

Table 2. Pulsars stronger than 5 mJy but not detected by the NVSS

PSR B	RA(2000) h m s	Dec(2000) ° ' "	$S_{1.4}$ mJy	Notes
1937+21	19 39 38.55	+21 34 59.1	16.0	Conf.
1800-21	18 03 51.35	-21 37 07.2	14.6	Scin.
2319+60	23 21 55.19	+60 24 30.6	12	Scin.
1845-01	18 48 24.00	-01 23 58.2	10	Scin.
2255+58	22 57 57.70	+59 09 14.9	9.2	Scin.
1839-04	18 42 26.49	-03 59 59.2	8.5	Conf.
1952+29	19 54 22.58	+29 23 17.9	8	Scin.
1815-14	18 18 23.79	-14 22 35.9	7.4	Scin.
1754-24	17 57 41.02	-24 21 56.8	7.1	Conf.
2011+38	20 13 10.49	+38 45 44.8	6.4	Scin.
1737-30	17 40 33.73	-30 15 41.9	6	Scin.
1919+21	19 21 44.80	+21 53 01.8	6	Scin.
1758-23	18 01 19.86	-23 06 16.8	5.7	Scin.
1849+00	18 52 28.00	+00 31 55.9	5.2	Scin.

the final images, i.e., over all the observation time and the bandwidth, so that

$$L_{nvss} = \sqrt{\left(\int_t Q\right)^2 + \left(\int_t U\right)^2}, \tag{1}$$

and

$$PA_{nvss} = \frac{1}{2} \frac{180}{\pi} \arctan\left(\frac{\int_t U}{\int_t Q}\right). \tag{2}$$

In pulsar observations, however, the total linearly polarized intensity is

$$L_{psr} \equiv \int_t \sqrt{Q^2 + U^2}, \tag{3}$$

and the polarization position angle PA is

$$PA_{psr} = \frac{1}{2} \frac{180}{\pi} \arctan\left(\frac{U}{Q}\right) \tag{4}$$

for each pulse longitude. The PA often swings more than 90° over a pulse. Since a positive value of Q or U in one part of a pulse may cancel a negative value in another part, it is believed that the pulsar emission is depolarized in continuum observations. Furthermore, the bandwidth depolarization occurs for pulsars with high rotation measures. Therefore the L/S in Table 1 should be taken as the lower limit of pulsar polarization.

Even so, pulsars are still the sources with the highest polarization compared to other kinds of objects (see Fig. 2). As seen from Table 1, some pulsars have very high linear polarization, such as PSRs B1742-30 ($L/S \sim 90\%$) and PSR B1929+10 ($L/S \sim 63\%$), even after the smearing and depolarization.

Since the NVSS has very accurate absolute position angle calibrations ($< 0.2^\circ$), the well measured PA of a few pulsars (with error $\lesssim 2^\circ$) may help to make an absolute PA calibration in pulsar observations. One example

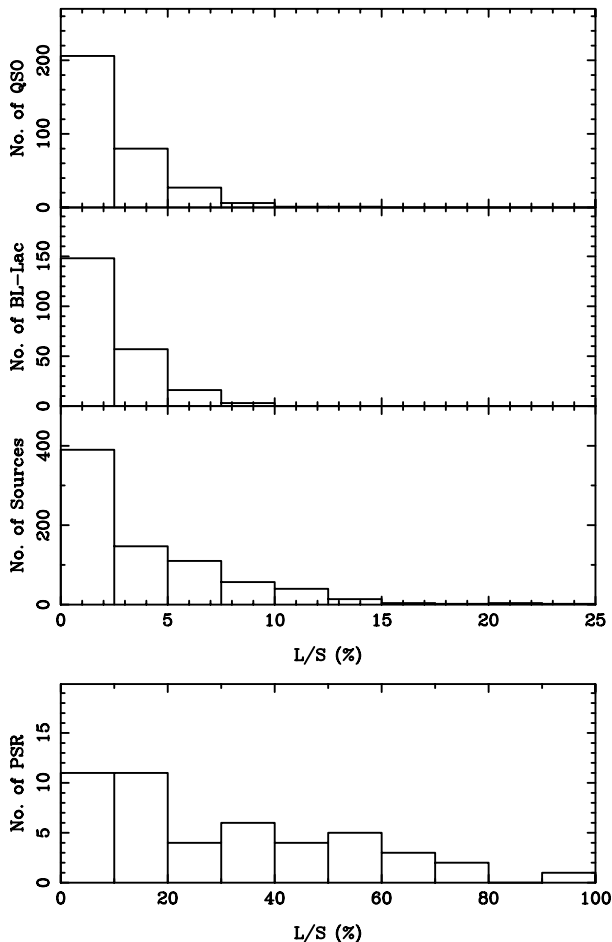


Fig. 2. Histograms of polarization percentage of a few kinds of objects: quasars, BL-Lac objects, all radio sources in one sky area, and pulsars. Note that the abscissa is up to 100% for pulsars, but just 25% for other objects

Table 3. Pulsar calibrators for absolute polarization angle

PSR J	PSR B	PA _{1400 MHz} ^{NVSS} (°)	RM (rad m ⁻²)
1932+1059	1929+10	46 ± 1	-6.1 ± 1.0
0742-2822	0740-28	-33 ± 1	150.4 ± 0.1
2022+5154	2021+51	11 ± 2	-6.5 ± 0.9
0543+2329	0540+23	-25 ± 2	8.7 ± 0.7
0630-2834	0628-28	-31 ± 2	46.2 ± 0.1

is shown in Fig. 3. First, using the VLA measurements of PA at 1400 MHz and the RM values, we calculated the averaged PA over the pulse at the observation frequency accordingly. Second, from the pulsar observations, we got PA for calibration pulsars using Eq. (2) from the pulse profiles (including interpulse if applicable) of Stokes parameters Q and U . Third we compared them to get an offset which represents the instrument PA offset, and used it to calibrate all pulsar observations.

In Table 3, we listed 5 pulsars which can be used for calibration purposes. All of them have strong linear polar-

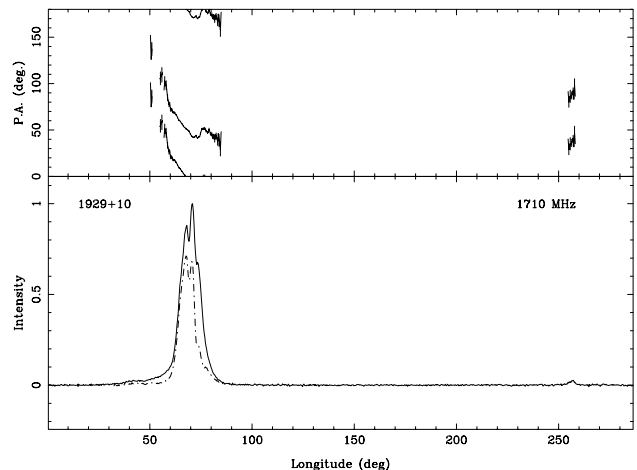


Fig. 3. Calibration for absolute polarization angle. Pulsar data were observed by von Hoensbroech & Xilouris (1997). In the lower panel, the total intensity, I , and linearly polarized intensity, L , are plotted with a thick continuum line and a dot-dash line, respectively. (The interpulse is almost 100% polarized.) In the top panel, the original PA data are plotted with a thin line (and with an error bar on every second point), and the calibrated PA data are plotted with a thick line

ized intensity that can be easily detected, and their rotation measures RM are either quite small ($\lesssim 10$ rad m⁻²) or accurately measured ($\sigma_{RM} \lesssim 1$ rad m⁻²). None of them has any mode-changing (e.g. PSR B1237+25 and PSR B1822+09) or complicated variations in PA across the profile (e.g. PSR B1933+16). All pulsars in Table 3 satisfy $\sigma_{PA} + \sigma_{RM} \cdot \delta(\lambda^2) < 3^\circ$, where $\delta(\lambda^2)$ was the difference of the wavelengths squared, and was taken as 1.0.

3.3. Proper motions

Pulsar proper motion is a very important quantity to be measured, so that pulsar velocities can be determined. Pulsar timing can be used to determine the proper motions of millisecond pulsars because of their great timing stability (e.g. Nice & Taylor 1995). However, for most pulsars, the proper motions can only be measured by determining the pulsar position precisely at two or more well-separated epochs using interferometry (e.g. Fomalont et al. 1997).

We compared the pulsar positions given in the pulsar catalog with those from the NVSS whose epoch is simply taken as MJD = 49718, and calculated pulsar proper motions if possible. The results are listed in Table 4. Pulsars with uncertainties of proper motion larger than 200 mas yr⁻¹ have been deleted. Because of the large uncertainty of the NVSS positions, we obtained only a few significant measurements: proper motion in declination direction of PSR B1133+16, and that in right ascension of PSRs B0823+26 and B2016+28. While the former two are consistent with the previous measurements made by

Table 4. Pulsar proper motions

PSR B	Δ RA arcsec	Δ Dec arcsec	Epoch MJD	$\mu_{\alpha} \cos \delta$ mas yr ⁻¹	μ_{δ} mas yr ⁻¹
0031-07	-2.53 ± 1.84	2.6 ± 1.9	40690	-102 ± 74	-105 ± 78
0329+54	-0.61 ± 0.44	0.9 ± 0.6	40105	-23 ± 16	34 ± 23
0450-18	-1.15 ± 1.01	-2.3 ± 1.0	46573	-133 ± 117	267 ± 116
0628-28	1.07 ± 1.21	-1.8 ± 1.2	40585	42 ± 48	71 ± 48
0740-28	-0.53 ± 0.80	-1.3 ± 0.8	46573	-61 ± 92	150 ± 93
0823+26	1.21 ± 0.94	-3.7 ± 1.0	40264	46 ± 36	-142 ± 38
0950+08	-0.15 ± 0.45	1.3 ± 0.6	46058	-14 ± 44	129 ± 59
1133+16	-0.29 ± 0.72	6.2 ± 0.8	42364	-14 ± 35	307 ± 40
1237+25	-0.54 ± 0.82	-1.0 ± 0.9	46460	-61 ± 91	-112 ± 100
1541+09	0.74 ± 1.49	-2.0 ± 1.5	42304	36 ± 73	-98 ± 74
1749-28	1.72 ± 0.53	-0.8 ± 0.9	40352	67 ± 20	31 ± 33
1818-04	-6.74 ± 2.69	-1.5 ± 2.7	40614	-270 ± 108	60 ± 108
1857-26	1.08 ± 0.95	1.7 ± 1.1	46573	125 ± 110	-197 ± 132
1933+16	-0.14 ± 0.58	-0.9 ± 0.7	40213	-5 ± 22	-34 ± 26
1946+35	-1.34 ± 2.56	-3.1 ± 2.9	42221	-65 ± 124	-151 ± 141
2016+28	3.y42 ± 0.79	0.4 ± 0.8	40105	130 ± 30	15 ± 30
2021+51	-0.46 ± 0.93	-0.6 ± 1.0	40614	-18 ± 37	-24 ± 40
2310+42	-2.75 ± 1.98	0.4 ± 1.4	43891	-172 ± 124	25 ± 87

Lyne et al. (1982), the latter one is marginally not. Cross-checking with Table 2 of Taylor et al. (1993), we found that all other measurements in Table 4 are consistent with (though poorer than) those given in the pulsar catalog, except for one new upper limit of PSR B0031-07. VLA A-array observations of these pulsars in **Table 1** should provide much more accurate positions, and hence could produce the first measurement of the proper motions of about 20 pulsars.

PSR B0031-07 is a nearby pulsar with distance 0.68 kpc. Its proper motion upper limit indicates that the pulsar has a velocity of 470 ± 346 km s⁻¹, quite normal according to the pulsar velocity distribution (Lyne & Lorimar 1994).

4. Summary

We identified about 97 strong pulsars from the NVSS catalog and presented the flux densities at 1.4 GHz. The parameters of linear polarization are independent, but slightly different (see Eqs. (1), and (2) above), measurements from those obtained from normal pulsar observations. Interstellar scintillation both helps and hinders the detection of pulsars. Table 1 presents all known pulsars detected by the NVSS. Well-calibrated VLA measurements of the average polarization angles of 5 strong pulsars can be used for *PA* calibrations for pulsar observations. By comparing the pulsar positions from the pulsar catalog and those from the NVSS, we got a proper motion upper limit of PSR B0031-07.

Acknowledgements. We thank the anonymous referee for his constructive suggestions which helped to revise the paper

significantly, and Drs. Dunc Lorimer, Elly Berkhuijsen, R. Wielebinski and Paul Arendt for their helpful comments. JLH is grateful for the hospitality of Prof. R. Wielebinski and Dr. R. Beck during his stay at the MPIfR, Bonn as an exchange scholar between the Chinese Academy of Sciences (CAS) and Max-Planck-Gesellschaft between 1997 May and 1998 August. He also thanks the National Natural Science Foundation of China and the Astronomical Committee of the CAS for continuous support.

References

- Bailes M., et al., 1997, ApJ 481, 386
Bartel N., Morris D., Sieber W., Hankins T.H., 1982, ApJ 258, 776
Condon J.J., Cotton W.D., Greisen E.W., et al., 1998, AJ 115, 1693
Cordes J.M., Chernoff D.F., 1998, ApJ 505, 315
Cordes J.M., Lazio T.J., 1991, ApJ 376, 123
Fomalont E.B., Goss W.M., Manchester R.N., Lyne A.G., 1997, MNRAS 286, 81
Gould D.M., Lyne A.G., 1998, MNRAS 301, 235
Gupta Y., Rickett B.J., Lyne A.G., 1994, MNRAS 269, 1035
Kaplan D.L., Condon J.J., Arzoumanian Z., Cordes J.M., 1998, ApJS 119, 75
Lorimer D.R., Lyne A.G., 1994, Nat 369, 127
Lorimer D.R., Yates J.A., Lyne A.G., Gould D.M., 1998, MNRAS 273, 411
Lyne A.G., Anderson B., Salter M.J., 1982, MNRAS 201, 503
Nice D.J., Taylor J.H., 1995, ApJ 441, 429
Prince T.A., Anderson S.B., Kulkarni S.R., Wolszczan A., 1990, Nat 346, 42
Taylor J.H., Manchester R.N., Lyne A.G., 1993, ApJS 88, 529
von Hoensbroech A., Xilouris K.M., 1997, A&AS 126, 121